Scanning Tunneling Microscopy Study of the Coverage-Dependent Structures of Pentacene on Au(111)

ARTICLE *in* LANGMUIR · FEBRUARY 2003

Impact Factor: 4.46 · DOI: 10.1021/la026221v

4 AUTHORS, INCLUDING:

Bruce A Parkinson
University of Wyoming
251 PUBLICATIONS **6,901** CITATIONS

SEE PROFILE

Scanning Tunneling Microscopy Study of the Coverage-Dependent Structures of Pentacene on Au(111)

C. B. France, P. G. Schroeder, J. C. Forsythe, and B. A. Parkinson*

Colorado State University, Department of Chemistry, Fort Collins, Colorado 80523

Received July 10, 2002. In Final Form: November 20, 2002

Pentacene thin films on Au(111) have been investigated at various coverages using scanning tunneling microscopy (STM) and temperature-programmed desorption (TPD). Two distinct binding environments, surface bound and bulk-like, were evident from TPD. The surface monolayer and multilayer pentacene molecules had binding energies of 110 and 106 kJ/mol, respectively. STM investigations of surfaces with pentacene coverages of around 0.25 monolayer equivalents (MLE) yielded four different ordered structures with end-to-end nearest neighbor interactions. Increasing the pentacene coverage from 0.25 to 1 MLE leads to ordered single monolayer films with rows of molecules aligned side-by-side. STM images of an annealed pentacene film revealed that these side-by-side rows are the dominant structure for complete monolayer films. A periodic row structure with a large spacing of 61 Å was observed to form in films with coverages greater than a monolayer (1.1−1.5 MLE). Upon deposition of 2 MLE, the widely spaced periodic row structure appears to be covered with a layer similar to the monolayer structure. STM images of these coverage-dependent structures and their relationship to bulk crystalline pentacene are discussed.

I. Introduction

The interface between organic semiconductors and metal contacts is important because charge transfer across this interface will be crucial for the operation of new organic-based devices. Ohmic behavior at these contacts is often desired but energetic and structural barriers can influence the electronic properties of the interface.[1] Therefore, it is useful to investigate the structural and energetic properties of these interfaces.

Pentacene single crystals have the highest field effect mobility found for an organic semiconductor.[2] Thin films of this material have been used for the fabrication of organic field-effect transistors on insulating oxide and plastic electrodes.[2] Gold has commonly been used for the source and drain contacts to the organic semiconductor layer or crystal; therefore, the structure of this interface is of interest. We have previously measured the energy level alignment of the pentacene/Au(111) interface using photoelectron spectroscopy, where a large interface dipole barrier was measured in the first layer of pentacene molecules.[3] Scanning tunneling microscopy (STM) studies of near monolayer coverages showed that molecules of pentacene on Au(111) form one-dimensional rows with the pentacene molecules aligning perpendicular to, or nearly perpendicular, to the row direction.[4] Similar structures were also found for pentacene on Cu(110) substrates.[5] Investigations of pentacene films with 1−1.5 monolayer equivalents (MLE) revealed a unique widely spaced periodic row structure.[6] Herein we report on the coverage-dependent structures formed by pentacene on Au(111) and the relationship between these structures and the bulk crystalline pentacene structure.

II. Experimental Section

Experiments were performed in a commercial Omicron Multiprobe ultrahigh vacuum (UHV) system (base pressure 5×10^{-11} mbar). This system is equipped with variable temperature scanning tunneling microscopy (VT-STM),[7] low-energy electron diffraction (LEED), X-ray and ultraviolet photoelectron spectroscopy (XPS and UPS) using a VSW EA125 single-channel hemispherical analyzer. Temperature-programmed desorption (TPD) has been added to the UHV system and is described below. A physical vapor deposition chamber (base pressure 1×10^{-9} mbar) is attached to the UHV system allowing sample and films to be prepared in situ.

The gold film was prepared by heating a 1 cm × 1 cm mica sample, attached to the sample plate using molybdenum clips, for 24 h in UHV at 300 °C to evaporate surface contaminants. Gold was then evaporated from a resistively heated tungsten basket onto the heated mica substrate.[8] The Mo clips provided an electrical contact to the gold surface during STM imaging. Sputter (3 keV Ar^+) and anneal (350 °C) cycles were used to clean and flatten the Au(111) surface. The chemical purity of the surface was determined with XPS (Mg Kα, 50 eV pass energy) and the presence of the $23 \times \sqrt{3}$ reconstruction was confirmed with STM.

Pentacene (Aldrich Chemical Co.) films were deposited under UHV (base pressure 1×10^{-9} mbar) from a resistively heated boron nitride crucible (source temperature, 142 °C). The source was maintained at 120 °C for 12 h prior to deposition to remove any volatile contaminants. Pentacene was then deposited at a rate of 4 Å/min as monitored by a Leybold quartz crystal microbalance (QCM). The Au(111) substrate was maintained at room temperature during the deposition.

The Au(111) surface was renewed for each experiment with a sputter and anneal cycle. Pentacene films with various thicknesses were then deposited on the cleaned surface. The STM images were obtained in a constant current mode with sample biases ranging from −2.0 to +2.0 V and tunneling currents between 0.1 and 0.5 nA. A background plane fit or slope correction

* Corresponding author. Fax: 970-491-1801. E-mail: bruce.parkinson@colostate.edu.

(1) Baldo, M. A.; Forrest, S. R. *Phys. Rev. B* **2001**, *64*.
(2) Dimitrakopoulos, C. D.; Purushothaman, S.; Kymissis, J.; Callegari, A.; Shaw, J. M. *Science* **1999**, *283*, 822.
(3) Schroeder, P. G.; France, C. B.; Park, J. B.; Parkinson, B. A. To be published.
(4) Schroeder, P. G.; France, C. B.; Park, J. B.; Parkinson, B. A. *J. Appl. Phys.* **2002**, *91*, 3010.
(5) Lukas, S.; Witte, G.; Wöll, C. *Phys. Rev. Lett.* **2002**, *88*, 028301.
(6) France, C. B.; Schroeder, P. G.; Parkinson, B. A. *Nano Lett.* **2002**, *2*, 693.
(7) The variable temperature capabilities of this instrument were not utilized during these experiments. All STM images in this report were produced at room temperature.
(8) The gold film thickness on the mica is estimated at a few micrometers.

10.1021/la026221v CCC: $25.00
Published on Web 00/00/0000 PAGE EST: 7.7

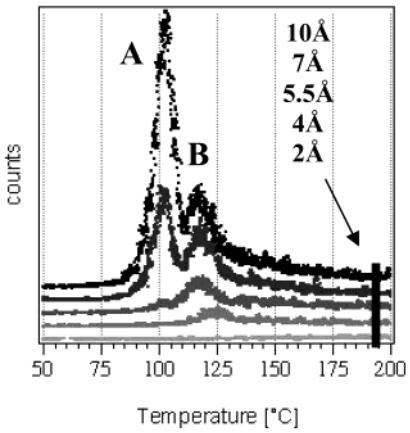

Figure 1. TPD spectra of pentacene desorbed from a Au(111) film. The bottom spectrum has 2 Å initial film coverage and the top 10 Å. Peak A originates from multilayer pentacene with a peak temperature of 106 °C and a binding energy of 106 kJ/mol. Peak B has a peak temperature of 120 °C and a binding energy of 110 kJ/mol and comes from monolayer pentacene on the Au(111).

was the only post collection processing applied to the images with the exception of Figures 3b and 8b, which were obtained from an FT averaging algorithm utilizing Scanning Probe Image Processing software (Image Metrology Aps.).

Temperature-programmed desorption experiments were performed by heating the sample using a resistive heater located directly behind the sample holder. The substrate surface temperature was measured using a Raytek Raynger MX IR thermometer. Emissivity values were determined using a calibration plot from a standard thermocouple with the sample holder at thermal equilibrium, giving the emissivity used for the Au(111) film of 0.12. The temperature was measured through an infrared transparent ZnSe window that is mounted on the UHV chamber. The signal from the IR thermometer is split and sent to a computer and a Eurotherm 2404 temperature controller. The Eurotherm temperature controller was used to control the heating rate (typically 15 °C/min) of the sample. Desorbed species were detected with a Stanford Research Systems quadrupole mass spectrometer (model RGA300) with an electron multiplier detector and ionization filament allowing for the detection of molecular fragments. The separation between the sample surface and the RGA is approximately 3 cm, with the substrate surface normal to the mass detector. The electron multiplier counts from a pre-selected mass are sent from the RGA to a computer. National Instruments Labview software is used on a PC computer to control, collect, and store temperature and mass count data as well as to plot the TPD spectrum. The Redhead equation[9] was used to determine the binding energy of a species based on the temperature of maximum desorption intensity.

III. Results and Discussion

TPD spectra for various pentacene coverages desorbed from a Au(111) film are shown in Figure 1, where the bottom spectra has the lowest initial coverage (2 Å) and the uppermost has the highest coverage (10 Å). TPD revealed two different binding environments at this interface. Due to nonlinearity of our quadrapole mass detector near its high mass limit, we measured the desorbed pentacene molecules at one-half their principal mass-to-charge ratio, which would correspond to a symmetrical fragment or a doubly charged molecule. Two peaks can be seen in the spectra of Figure 1 (labeled A and B) indicating that there are two different adsorbate environments present. Peak A in Figure 1 is only present for coverages greater than 5 Å and has a peak temperature of 106 °C, corresponding to a calculated binding energy of 106 kJ/mol. Investigation of different coverages of pentacene on Au(111) found that the intensity of peak A increased with increasing initial film thickness. In conjunction with STM analysis of these films before TPD, it was determined that the signal from peak A originates from a multilayer environment where the interaction is exclusively from other pentacene molecules and so represents the sublimation energy of pentacene. Peak B is seen in all of the spectra, including the 2 Å spectrum and has a peak temperature of 120 °C and calculated binding energy of 110 kJ/mol. The peak is always found at low coverages and its intensity saturates at coverages above 5 Å. STM analysis of pentacene films, where only peak B is present in the TPD spectra, showed only monolayer and submonolayer structures on the surface. Therefore peak B is attributed to the initial monolayer of pentacene on the Au(111) surface. This monolayer−multilayer distinction allowed TPD to be used to determine the film coverage in further investigations of this interface. It is also noteworthy that we observed a large (0.95 eV) initial work function shift in the orbital alignment of pentacene on Au(111), with the majority of the shift occurring within the first 4 Å of deposition.[3,4] This work function shift is attributed to donated electron density from the pentacene molecules to the Au(111). The increased interaction between the first pentacene layer and the Au(111) is likely the cause for the larger binding energy of the submonolayer film on the surface, as determined with TPD (4 kJ/mol greater than multilayer films). This stronger binding at lower coverages is also evident by peak B shifting to higher binding energies at lower film coverages, which would correspond to an increased interaction at lower coverages which is consistent with the initial work function shift.[3] Therefore, at lower pentacene coverages more electron density per molecule is donated from the organic film to the Au(111) thus increasing the interaction between the two species at the interface.

Scanning tunneling microscopy was used to investigate the structures formed by pentacene molecules on the Au(111) surface. Four distinct structures were observed after deposition of about 0.25 MLE of pentacene. None of these four low-coverage structures lifted the Au(111) $23 \times \sqrt{3}$ reconstruction which was simultaneously observed in many STM images. The reconstruction was useful for calibrating the size of the structures and to identify their orientation with respect to the Au substrate lattice. The lowest coverage structure observed is labeled type 1 and is shown in a 25.4 nm × 28.7 nm STM image, (Figure 2A). Pentacene molecules in the type 1 structure form paired rows where the pentacene molecules align perpendicular to the Au(111) $23 \times \sqrt{3}$ reconstruction (as observed in other STM images). Each molecule interacts with its nearest neighbor in an end-to-end fashion. The center-to-center distance between the pentacene molecules in the end-to-end rows is 18 ± 1 Å. The separation between the two rows of pentacene molecules that make up the paired row is 13 ± 1 Å, the repeating distance between the paired rows is 32 ± 1 Å, and the measured unit cell angle is $86 \pm 3°$. Continued imaging with the STM tip tended to disrupt the ordering of this structure. Common disruptions include pushing together or separating molecular rows that previously were paired with other rows. In addition, many disordered or "noisy" areas in the images were observed and attributed to the STM tip disrupting the loosely packed (low-coverage) structure. Figure 2B shows a proposed model of the paired row structure, which is aligned with the STM image as indicated by the directional vectors. All figures with directional vectors will be aligned for all models and STM images in the figure.

(9) Redhead, P. A. *Vacuum* **1962**, *12*, 203.

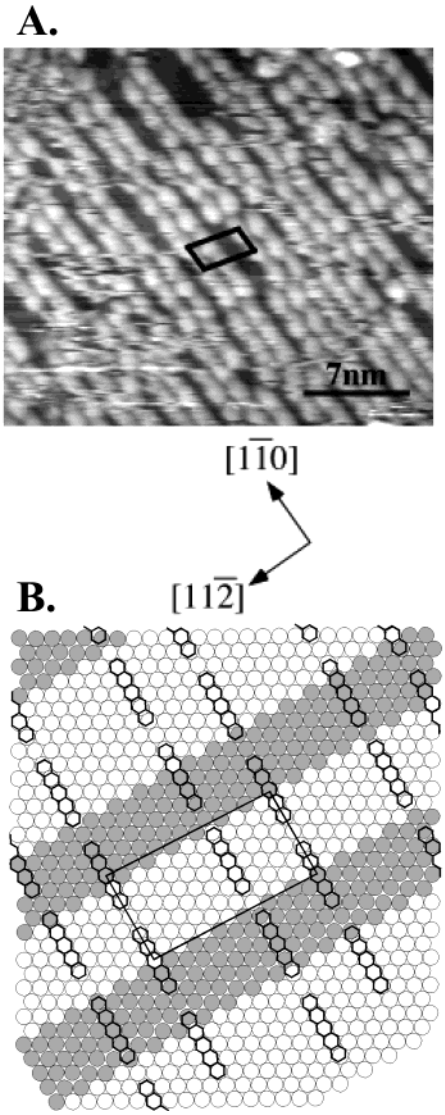

Figure 2. (A) A 25.4 nm × 28.7 nm STM image of the low-coverage type 1 pentacene structure. (−2.0 V, 0.3 nA) (B) A proposed model of the pentacene ordering in the $6 \times \sqrt{127}$ type 1 structure. The dark substrate atoms represent the elevated $23 \times \sqrt{3}$ reconstruction of the Au(111). The directional vectors for the Au(111) are consistent for the model and STM image.

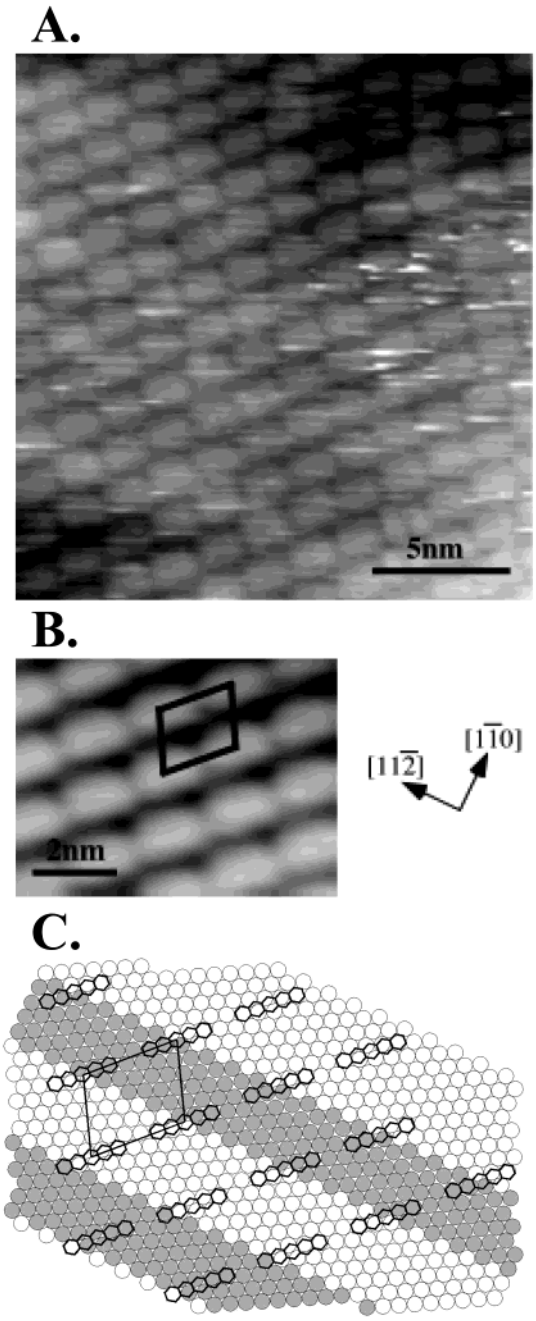

Figure 3. (A) A 18.7 × 18.7 nm STM image of type 2 ordering on Au(111). (−2.0 V, 0.3 nA) (B) An averaged STM image produced from Figure 3A using SPIP software. The pentacene unit cell is drawn has been added. (C) A model of the pentacene in the $3\sqrt{3} \times \sqrt{19}$ type 2 overlayer. The Au(111) directional vectors are consistent for the entire figure.

The long axis of the pentacene molecules is aligned perpendicular to the gold reconstruction [11$\bar{2}$], represented by the dark substrate atoms. It is important to note that in the model shown in Figure 2B and all subsequent models, the actual position of the molecules with respect to the substrate Au atoms has not been directly observed but is based on the expected location as will be discussed below. This structure corresponds to an unusual $6 \times \sqrt{127}$ (17.3 × 32.4 Å) noncentrosymmetric overlayer unit cell with a theoretical packing density of 3.57×10^{13} molecules/cm^2 and a unit cell angle of 87.5°. The reason for the pairing of the pentacene rows is unclear since there is sufficient room for pentacene molecules to adsorb between the paired rows as was seen after STM tip disruption of the structure and is shown in the proposed model.

An 18.7 × 18.7 nm STM image in Figure 3A shows the type 2 structure. The Au(111) $23 \times \sqrt{3}$ reconstruction, [11$\bar{2}$], is observed beneath this structure running nearly vertical across the image as depicted by the directional vectors. A unit cell averaged 5.6 × 7.6 nm STM image is shown in Figure 2B along with the observed unit cell. The experimentally measured unit cell distance between the pentacene molecules (center-to-center) in the end-to-end rows is 18 ± 1 Å with a unit cell distance of the side-by-side molecules of 15 ± 1 Å and a unit cell angle of 105 ± 3°. A proposed model of this structure is shown in Figure 3C where the pentacene molecules form a $3\sqrt{3} \times \sqrt{39}$ (15.0 × 18.0 Å) unit cell with $\alpha = 106.1°$ (unit cell angle) with a theoretical packing density of 3.7×10^{13} molecules/cm^2.

Figure 4A shows a 50 nm × 50 nm STM image of the type 3 low-coverage structure. The structures in the upper left of Figure 4A are side-by-side rows or single molecular width rows that will be discussed below. The lower left of the image contains two polymorphic structures where the left side shows type 1 ordering while the molecules on the

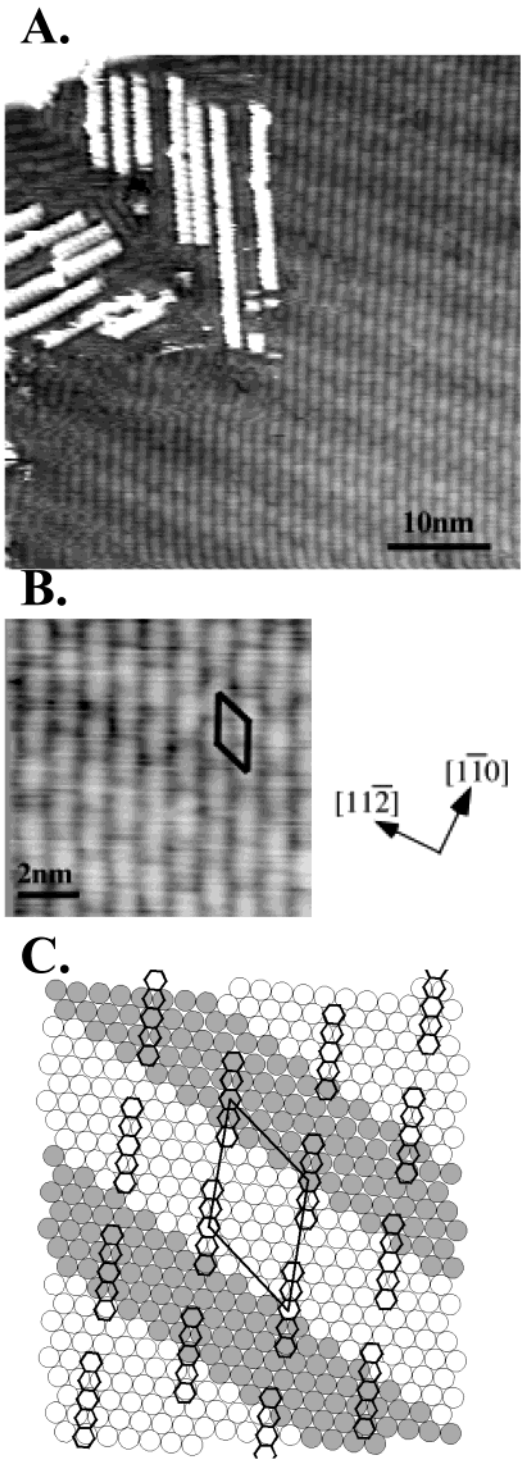

Figure 4. (A) A 50 × 50 nm STM image with 3 different pentacene polymorphs. The upper left contains side-by-side row pentacene. The lower left contains the type 1 low-coverage structure. Molecules on the right side of the image are the type 3 structure. (−2.0 V, 0.3 nA) (B) A 9.9 × 10.1 nm zoom-in of the type 3 structure with the pentacene unit cell drawn. (B) A proposed model of the $2\sqrt{7} \times \sqrt{37}$ type 3 structure.

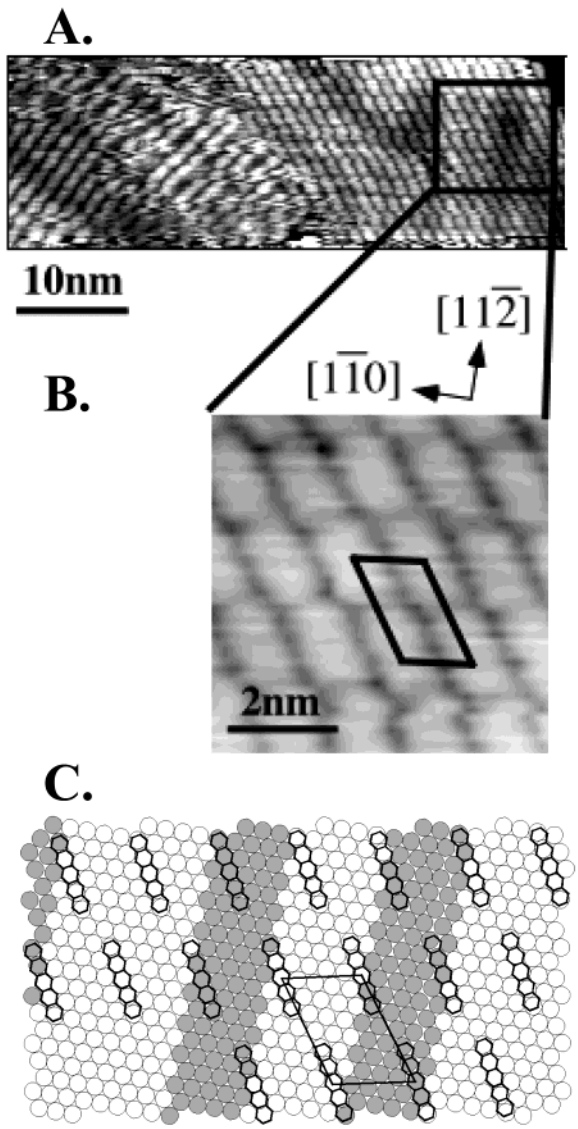

Figure 5. (A) A 17 × 48 nm STM image of two different pentacene polymorphs on Au(111). The left half of the image contains the type 1 pentacene structure with the Au reconstruction running perpendicular to the pentacene molecules. On the right side of the image is the type 4 polymorph with a Au reconstruction elbow visible. (−2.0 V, 0.3 nA) (B) A 6.1 nm × 6.1 nm zoom in from the upper right of Figure 5A. The directional vectors are consistent for this location (Figure 5B location) and the proposed model. The pentacene unit cell has been included. (C) A proposed model of the $\sqrt{21} \times \sqrt{43}$ type 4 ordering.

right side of the image are the type 3 structure. By averaging measurements of many STM images it was determined that the pentacene molecules in the type 3 structure have a center-to-center distance of 17 ± 1 Å in the end-on-end row direction and 13 ± 1 Å center-to-center separation that determines the other unit cell dimension, $\alpha = 51 \pm 3°$. A close-up STM image (9.9 nm × 10.1 nm) showing the pentacene unit cell and Au directional vectors for the figure is presented in Figure 4B. A proposed model of the type 3 structure is offered in Figure 4C where a $2\sqrt{7} \times \sqrt{37}$ (15.3 × 17.5 Å) with $\alpha = 52.8°$ pentacene unit cell was found with a theoretical packing density of 3.73×10^{13} molecules/cm^2.

The type 4 low-coverage ordering is shown in the 17 × 48 nm STM image of Figure 5A where the left half of the image is the type 1 structure and the type 4 structure is seen on the right side. The Au(111) reconstruction is present under both polymorphs with a reconstruction elbow located under the type 4 structure and perpendicular to the direction of the type 1 rows, as described above. To help clarify the pentacene orientation relative to the Au(111), a close-up STM image is shown in Figure 5B from a location in Figure 5A where the Au reconstruction is uniform. The pentacene unit cell is drawn in Figure 5B for clarity. The directional vectors are oriented to this

zoomed in location and the model. End-to-end interactions between nearest neighbor molecules resulted in measured distances, center-to-center, of 18 ± 1 Å between end-on molecules and 13 ± 1 Å between side-on molecules, α = 113 ± 3°. The type 4 structure has been determined to have a $\sqrt{21} \times \sqrt{43}$ (13.2 × 18.9 Å) unit cell, α = 116.7°, with a theoretical packing density of 4.00×10^{13} molecules/cm^2. A model of this overlayer is shown in Figure 5C.

As discussed above, these type 1−4 structures were measured at submonolayer film thickness (~0.25 MLE). As seen in many of the figures of this report, multiple structures were often imaged in the same STM image with as many as 4 polymorphs coexisting in an area of 2500 nm^2. The interesting end-to-end interaction between neighboring pentacene molecules in these low-coverage structures is unexpected. Crystal structures of pentacene show the molecules aligning in a herringbone structure with nearest neighbor molecules in a side-by-side fashion and layers of the molecules tilted to facilitate edge-face interactions.[10−12] Pentacene polymorphs on Au(111) have yielded structures similar to these bulk orientations, as was observed in previous STM experiments.[4] In those experiments, pentacene films with a thickness of ~0.75 MLE were found to form rows with nearest neighbors having side to side interactions. At these higher coverages, side-by-side rows allow for an increased overlayer packing density on the Au(111). Statistical analysis of the row spacings revealed the formation of 3 basic orientations of side-by-side rows, type A ($2 \times 3\sqrt{3}$), type B ($2 \times 2\sqrt{7}$), and type C ($2 \times \sqrt{31}$) unit cells. Rows separated by one or more additional Au atom were also observed, increasing the area covered by each unit cell.

Coverages close to one monolayer were investigated by depositing approximately 10 Å of pentacene on the gold surface and annealing the sample at 60 °C for around 15 min. After annealing, the STM was used to investigate the ordered structures at room temperature. TPD was subsequently performed to estimate the thickness of the remaining film. STM experiments revealed that multilayer films remained on parts of the surface after annealing, however large areas of the surface showed only the annealed monolayer. A 300 nm × 300 nm STM image, shown in Figure 6A, demonstrates the types of structures seen on an annealed pentacene film on the gold surface. A zoom-in of a region from Figure 6A is shown in Figure 6B. The directional vectors for the Au(111) are included for the zoomed-in region and the locations of the monolayer and multilayer pentacene structures are highlighted. The Au(111) $23 \times \sqrt{3}$ reconstruction is observed throughout the image, through both the first (darker regions) and second layer (brighter areas) pentacene structures. A Au(111) screw dislocation begins in the center of the image, rotating out from the origin in a counterclockwise direction. The bright rows of pentacene molecules are single molecule width rows with the molecules aligning side-by-side. Upon zooming in on the monolayer covered areas, two pentacene polymorphs were identified. The first structure identified was the $2 \times 2\sqrt{7}$ (5.76 × 15.3 Å), α = 79.1°, structure with a theoretical packing density of 1.14×10^{14} molecules/cm^2, originally identified as the type B unit cell in our previous paper where the initial pentacene coverage was 0.75 MLE but annealing was not performed.[4] The type B monolayer is shown in the STM image in Figure 7A where

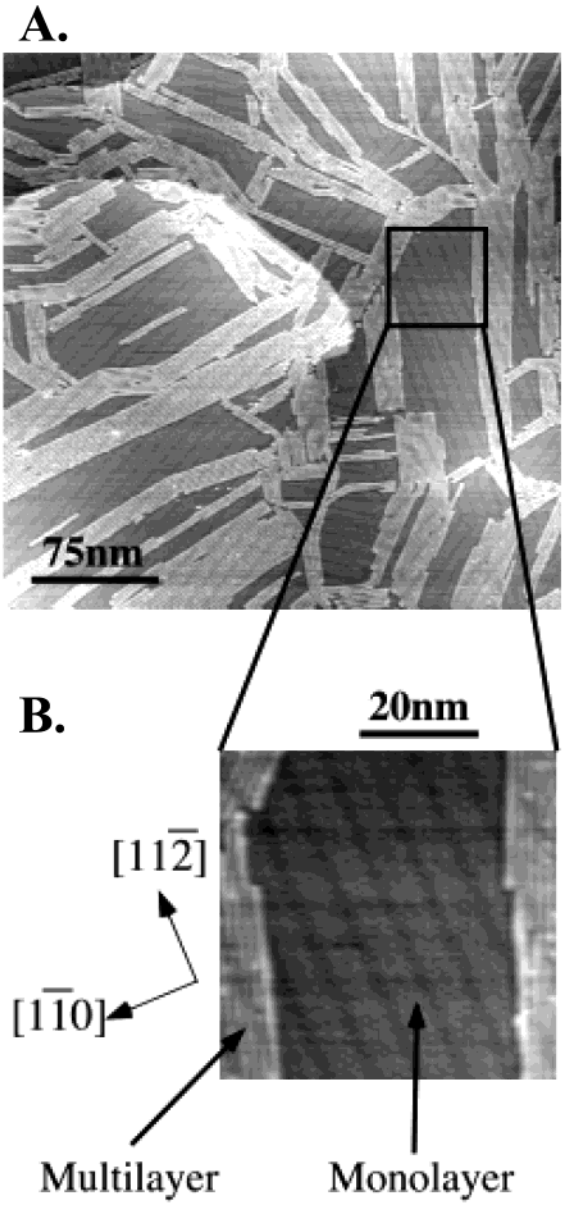

Figure 6. (A) A 300 nm × 300 nm STM image of an annealed pentacene film on Au(111). A screw dislocation is observed coming from the center of the image in a counterclockwise direction. The Au $23 \times \sqrt{3}$ reconstruction is imaged through both the first and second layer pentacene structures. (−2.0 V, 0.3 nA) (B) A zoom of the indicated region from Figure 6A with corresponding directional vectors. Bright second layer rows of pentacene molecules are shown with a monolayer of pentacene molecules visible throughout the image.

the gold reconstruction can clearly be seen under the monolayer structure. The measured center-to-center distances between the pentacene molecules in the overlayer are 6 ± 1 Å for the side-to-side molecules and 15 ± 1 Å for molecules aligned end-to-end (α = 79 ± 3°). A proposed model of the type B monolayer is shown in Figure 7B. The other monolayer unit cell was also previously identified in submonolayer films (~0.75 MLE) as the type C unit cell.[4] This type C structure was identified as a $2 \times \sqrt{31}$ (5.76 × 16 Å), α = 69.0°, unit cell with a packing density of 1.09×10^{14} molecules/cm^2. In Figure 8A, an image of the type C monolayer structure is shown in a 12.4 nm × 12.4 nm STM image. The measured overlayer distances of the pentacene molecules are 15 ± 1 Å for the end-to-end molecules and 6 ± 1 Å for the side-to-side molecules (α = 75 ± 3°). An averaged image of this type

(10) Siegrist, T.; Kloc, C.; Schön, J.; Batlogg, B.; Haddon, R.; Berg, S.; Thomas, G. *Angew. Chem., Int. Ed.* **2001**, *40*, 1732.
(11) Campbell, R. B.; Robertson, J. M.; Trotter, J. *Acta Crystallogr.* **1961**, *14*, 705.
(12) Campbell, R. B.; Robertson, J. M.; Trotter, J. *Acta Crystallogr.* **1962**, *15*, 289.

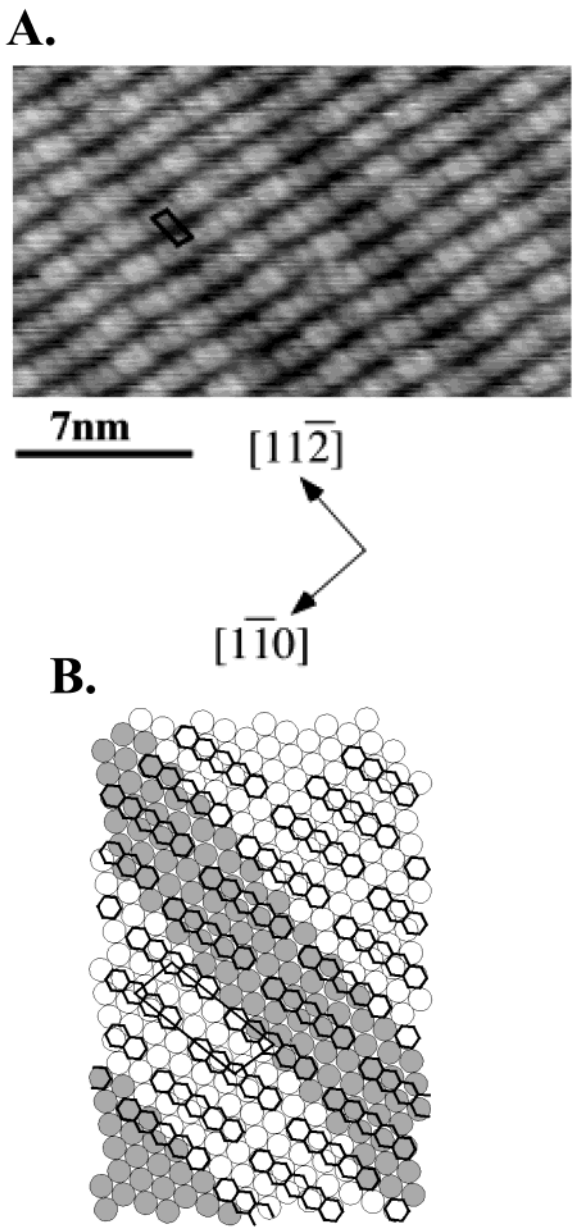

Figure 7. (A) The type B monolayer is shown in the constant current STM image. (−2.0 V, 0.5 nA) (B) A proposed model of the $2 \times 2\sqrt{7}$ type B monolayer structure which has been aligned with the STM image.

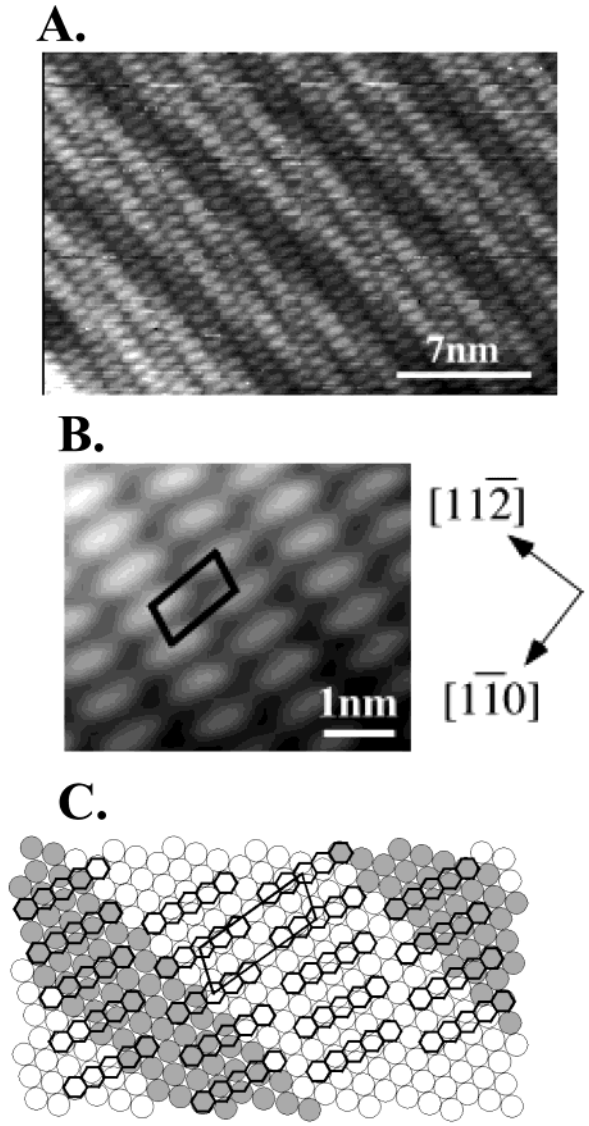

Figure 8. (A) A 27 × 27 nm STM image of the type C monolayer structure on Au(111). (−2.0 V, 0.4 nA) (B) An averaged STM image from Figure 8A with pentacene unit cell added. (C) A model of the $2 \times \sqrt{31}$ type C monolayer aligned with directional vectors as indicated.

Table 1. Modeled (bold) and Experimentally Determined Unit Cell Information for Submonolayer and Monolayer Pentacene Structures on Au(111)

structure	a	b	α	density (mlcs/cm^2)	unit cell symmetry
Type 1	**17.3 Å**	**32.4 Å**	**87.5°**	**3.57×10^{13}**	P1
	18 ± 1 Å	32 ± 1 Å	86 ± 3°		
Type 2	**15.0 Å**	**18.0 Å**	**106.1°**	**3.70×10^{13}**	P2
	15 ± 1 Å	18 ± 1 Å	105 ± 3°		
Type 3	**15.3 Å**	**17.5 Å**	**52.8°**	**3.73×10^{13}**	P2
	13 ± 1 Å	17 ± 1 Å	51 ± 3°		
Type 4	**13.2 Å**	**18.9 Å**	**116.7°**	**4.00×10^{13}**	P2
	13 ± 1 Å	18 ± 1 Å	113 ± 3°		
Type A	**5.76 Å**	**15.0 Å**	**90°**	**1.16×10^{14}**	P2mm
Type B	**5.76 Å**	**15.3 Å**	**79.1°**	**1.14×10^{14}**	P2
	6 ± 1 Å	15 ± 1 Å	79 ± 3°		
Type C	**5.76 Å**	**16.0 Å**	**69°**	**1.09×10^{14}**	P2
	6 ± 1 Å	15 ± 1 Å	75 ± 3°		
Type D	**5.76 Å**	**18.0 Å**	**76.1°**	**9.64×10^{13}**	P2
Type E	**5.76 Å**	**20.8 Å**	**73.9°**	**8.35×10^{13}**	P2

C structure is shown in Figure 8B, as produced by SPIP software. The overlayer unit cell has been drawn in to clarify the pentacene positions. A model aligned with the STM images and showing the rows of pentacene molecules in the type C monolayer is presented in Figure 8C. The fact that these two unit cells predominate on the annealed monolayer film indicates they are most likely the stable configurations for a monolayer structure. Table 1 summarizes all of the ordered monolayer and submonolayer structures described in this report. The labeling of these structures is somewhat arbitrary but numbers are used for the low-coverage structures ($<8 \times 10^{13}$ cm^{-2}) with end-to-end interactions and letters are used for the high-coverage structures ($>8 \times 10^{13}$ cm^{-2}) with side-on interactions.

It is interesting to compare the observed monolayer structures with the molecular packing in pentacene crystals. The molecular packing along the (100) plane of the crystal is very similar to the structure of the type B monolayer. Figure 9 shows 4 × 4 unit cells of the (100) face of the bulk pentacene structure from a crystal structure determination (compare with Figure 7B).[11] It is

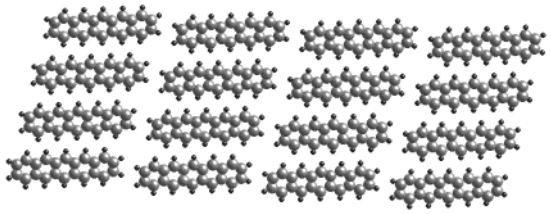

Figure 9. 4 × 4 unit cells of the crystalline pentacene structure at the (100) plane. These molecules are not coplanar with the (100) plane; however, they have a structure very similar to that of the type B monolayer.

important to note that the molecules in Figure 9 are not completely coplanar with the (100) plane as they are expected to be on the Au surface. Even so, the unit cell distances of 6.1 × 16.0 Å and unit cell angle of 78° are within experimental error of the type B monolayer distances 6 ± 1 Å × 15 ± 1 Å and angle 79 ± 3°. The type C monolayer structure does not resemble the bulk structure of either pentacene polymorph and therefore its existence is attributed to a favorable adsorbate−substrate interaction. Epicalc[13] was used to investigate the presence of any epitaxial interactions between these monolayer structures and the reconstructed Au(111) substrate. The type B monolayer was found to be coincident with the reconstructed substrate whereas the type C monolayer was found to be incommensurate with the reconstructed Au(111) surface. The coincidence of the type B monolayer and its structure similar to that of bulk pentacene suggests that it could be the template layer for the direct formation of bulk pentacene crystallites with the (100) planes parallel to the Au(111) substrate.

Investigation of the pentacene film on Au(111) at greater than monolayer coverage led to the discovery of a unique widely spaced periodic (WSP) row structure.[6] Rows made up of tilted pentacene molecules formed with a periodic center-to-center distance of 61 ± 5 Å, an unusually large separation as it is significantly larger than the width of the pentacene molecules. STM images after deposition of ∼1.5 MLE of pentacene revealed WSP rows covering the entire investigated surface. The nonbulk-like, incommensurate type C monolayer was found to lie below these unique structures with the WSP rows traveling across the surface coincident with the monolayer structure. The large spacing of the WSP rows was attributed to the incommensurate type C monolayer forming defects or offsets allowing for better alignment with the reconstructed surface. Epicalc determined that the large WSP overlayer was coincident with the reconstructed substrate. Details of this structure are published elsewhere.[6]

Two monolayer equivalents or 10 Å pentacene films were also imaged with STM. Observation of the thicker films was more difficult because of mobile, less strongly bound, pentacene molecules in the second layer, thus leading to significant noise and streaking in the STM images. However, some observations revealed that the WSP row molecules were being covered with another layer of side-by-side pentacene rows, similar to the structures found in the monolayer films. While the precise alignment of the pentacene molecules was not determined in these films, an additional layer of pentacene molecules aligning with their aromatic plane parallel to the substrate is similar to what would be expected of crystalline ordering. This additional layer would generate parallel-tilted-parallel herringbone structure similar to the crystalline pentacene structure growing from the (100) plane on the Au(111).

High-resolution STM images of pentacene in the side-by-side row structures commonly showed individual molecules as having more facile tunneling at either end of the molecule. An excellent example of this was shown in a previously published high-resolution STM image[14] where side-by-side pentacene rows clearly show each pentacene molecule consists of bright lobes at either end of the molecule. Similar high-resolution images were also frequently obtained during the studies reported herein with sample biases ranging from −2 to 2 V. The lack of a strong voltage dependence on the molecular contrast suggests that pentacene molecular orbitals do not dominate the tunneling during the imaging process. The angle of the pentacene rows and molecule directions measured with respect to the Au(111) 23 × $\sqrt{3}$ reconstruction and the size of the pentacene molecule relative to the Au lattice suggest that the interaction between the Au substrate atoms and pentacene dominates the STM image contrast. Although we do not have direct evidence of this interaction, many of the models presented in this report show the pentacene molecule aligning with the two end acene rings on atop sites of the Au lattice, while the middle ring of the molecule resides above a 2-fold site. If this alignment is correct, we believe there will be more facile tunneling to the region of the pentacene molecules that are above the atop sites of the Au lattice while the middle of the molecule will not interact as strongly with the substrate as it straddles a Au 2-fold site. A similar double-lobed STM contrast mechanism has been proposed for very low coverages of pentacene on a Si(100) 2 × 1 surface.[15] Higher-resolution images of the low-coverage pentacene structures on the Au(111) surface do not show a double-lobed structure, instead showing uniform tunneling across the entire molecule. We believe this is due to thermal motion of the molecules in the low packing density, end-on-end structures. The space around each pentacene molecule in the lower density films allows limited rotational and lateral motion that prevents submolecular resolution of the molecules at room temperature and results in averaging of the tunneling current across the molecule. Although the angles of the substrate reconstruction, relative to the direction of the pentacene molecules, indicate the molecules are lining up with the substrate as discussed above, motion of the pentacene causes a blurring of the molecules during the STM imaging process and thus the molecules appear larger than expected (for example, see Figure 3A). Low-temperature STM studies are being attempted to further understand the Au−pentacene interactions and image contrast mechanisms in these low-coverage films.

A summary of the many structures identified and the coverages at which they were imaged is presented in Table 1 along with a film thickness vs structure chart shown in Figure 10. The bottom axis of Figure 10 is the pentacene film thickness in angstroms, as determined by quartz crystal microbalance, and monolayer coverage as confirmed from STM and TPD measurements. The four low-coverage structures, types 1−4, all had end-on-end nearest neighbor interactions. Whereas the higher-coverage side-by-side row structures are the unit cells of types A−E. Type D unit cells have 2 Au atoms between side-by-side rows and type E unit cells have more than two Au atoms between rows; for more information on the type A, D, and

(13) Epicalc is a computer program that performs epitaxy calculations utilizing an analytical algorithm. Epicalc was developed by the Ward group in the department of Chemical Engineering at the University of Minnesota and is available at http://www.wardgroup.umn.edu/software.html.

(14) Figure 4 of ref 4.

(15) Kasaya, M.; Tabata, H.; Kawai, T. *Surf. Sci.* **1998**, *400*, 367.

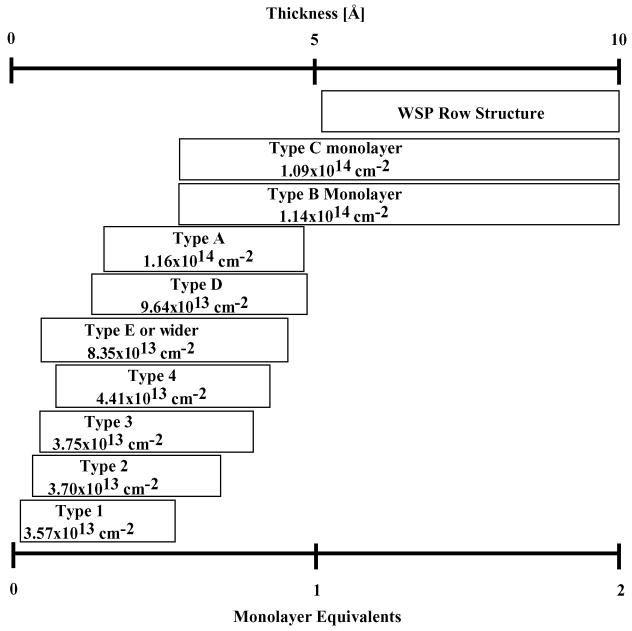

Figure 10. A film thickness vs structure diagram of the ordered pentacene polymorphs formed on Au(111). The bottom axis is the coverage of the pentacene molecules in monolayer equivalents and angstroms, as determined by quartz crystal microbalance.

E structures see ref 10. Type E or wider (many Au atoms between rows) are the first side-by-side row structures found at lower coverages. Increasing the film thickness forces the rows together and generates additional side-by-side rows until a monolayer film is produced. Additional deposition of pentacene generates the tilted molecule WSP rows that cover the entire surface. Continued deposition of pentacene, around two monolayers, covers the WSP rows with a structure that appears to be similar to the side-by-side rows of the monolayer.

It is worth noting the unexpected richness of observed structures that have been imaged at this interface. The surprising number of ordered structures formed by this nonpolar, polyacene molecule was not expected on the relatively inert Au surface. The structural change between the end-on to side-on interactions in the film results in a sudden two and a half-fold increase in the packing density between the low-coverage structure (type 4) and the monolayer structures (type B and C), see Table 1. While two distinct types of structures were imaged (end-on and side-on), the many slight variations observed suggest a small energy difference or concentration dependence between those structures. The existence of pentacene 3D crystalline polymorphs also points out that subtle structural differences are possible when packing molecules with primarily van der Waals interactions.[10,11] These results indicate the interesting and complex nature of this technologically interesting interface and the need for additional investigation into these types of systems.

IV. Summary

The coverage-dependent ordered structures of pentacene molecules on Au(111) have been investigated. Temperature-programmed desorption was used to determine the presence of two distinct binding environments—the monolayer and multilayer—with binding energies of 110 and 106 kJ/mol, respectively. TPD was also used to calibrate the coverage of the pentacene film where 5 Å was determined to be the thickness of one monolayer. Scanning tunneling microscopy was utilized to image the ordered structures of pentacene on the reconstructed Au(111) surface. At low coverages of pentacene, four end-to-end nearest neighbor ordered structures were identified. Increasing the pentacene coverage generated structures where the higher packing density side-by-side rows became dominant as film thickness approached one monolayer. Two different monolayer structures were identified after annealing films with greater than a monolayer coverage. From these two monolayer structures, the type B form was found to have parameters similar to the bulk (100) form of pentacene and was coincident with the reconstructed substrate. The type C form was found to be incommensurate with the reconstructed Au(111) and had geometries substantially different than that of the bulk pentacene structures. Evidence for the formation of defects or offsets in the type C film to allow for a coincident interaction is demonstrated through the adhering of additional pentacene molecules at these sites and the formation of the WSP rows. The large number of ordered structures formed by this nonpolar, aromatic pentacene molecule on the relatively unreactive Au(111) substrate is quite surprising and underscores the complexity of this heterojunction.

Acknowledgment. This work is supported by the Department of Energy under Contract DE-F603-96ER14625.

LA026221V